R. Jimbo[1]*, P.G. Coelho[2],
M. Bryington[3], M. Baldassarri[2],
N. Tovar[2], F. Currie[4], M. Hayashi[1],
M.N. Janal[5], M. Andersson[6], D. Ono[7],
S. Vandeweghe[1,8], and A. Wennerberg[1]

[1]Department of Prosthodontics, Faculty of Odontology, Malmö University, Sweden; [2]Department of Biomaterials and Biomimetics, New York University, New York, USA; [3]Division of Restorative and Prosthetic Dentistry, The Ohio State University College of Dentistry, Columbus, Ohio, USA; [4]Promimic AB, Gothenburg, Sweden; [5]Department of Epidemiology and Health Promotion, New York University College of Dentistry, New York, USA; [6]Department of Chemical and Biological Engineering, Applied Surface Chemistry, Chalmers University of Technology, Gothenburg, Sweden; [7]Division of Applied Prosthodontics, Nagasaki University Graduate School of Biomedical Sciences, Nagasaki, Japan; and [8]Department of Periodontology and Oral Implantology, Dental School, Faculty of Medicine and Health Sciences, University of Ghent, Belgium; *corresponding author, ryo.jimbo@mah.se

Nano Hydroxyapatite-coated Implants Improve Bone Nanomechanical Properties

ABSTRACT

Nanostructure modification of dental implants has long been sought as a means to improve osseointegration through enhanced biomimicry of host structures. Several methods have been proposed and demonstrated for creating nanotopographic features; here we describe a nanoscale hydroxyapatite (HA)-coated implant surface and hypothesize that it will hasten osseointegration and improve its quality relative to that of non-coated implants. Twenty threaded titanium alloy implants, half prepared with a stable HA nanoparticle surface and half grit-blasted, acid-etched, and heat-treated (HT), were inserted into rabbit femurs. Pre-operatively, the implants were morphologically and topographically characterized. After 3 weeks of healing, the samples were retrieved for histomorphometry. The nanomechanical properties of the surrounding bone were evaluated by nanoindentation. While both implants revealed similar bone-to-implant contact, the nanoindentation demonstrated that the tissue quality was significantly enhanced around the HA-coated implants, validating the postulated hypothesis.

INTRODUCTION

The current trend for biomaterial modification has a specific goal: in principle, to enhance bioactivity for functional and structural replacement of the native organ. Throughout the history of biomedical engineering, we have learned that mimicking biology would be the ultimate modification, and hierarchical biomimetic architecture has led to the creation of different functional elements (Alberts *et al*., 2002). Nanoscale alterations have been suggested to increase its bioactivity (Goransson *et al*., 2009), and it is now evident that various molecular interactions occur at this size level (Dalby *et al.*, 2002).

Nanostructures applied to biomaterials have been suggested to contribute to a higher grade of osseointegration (Ellingsen *et al.*, 2004), and it has been shown that biology responds sensitively to different nanostructures (Coelho *et al.*, 2011; Jimbo *et al.*, 2012). In fact, Webster and Ahn specified that nanostructures smaller than 100 nm are most effective in cellular integration and suggested that these should be differentiated from the so-called 'submicron' structures (Webster and Ahn, 2007). What is unique about the effect of HA nanocoating is that the stimulatory outcomes are related not only to the topography, but also to the effect of chemistry, which generates a synergetic effect (Jimbo *et al*., 2012). Further, compared with the traditional 'thick' HA coatings, which have been reported to generate clinical problems (Albrektsson, 1998), the mono-layered thin HA coating seems to be stable and shows no signs of foreign body reaction (Jimbo *et al.*, 2012).

In a previous study of gene expression around turned-nano HA-coated implants, the nano HA coating significantly enhanced osteogenic gene expression while increasing osteoclastic activity, suggesting that the nano HA is actively involved in bone formation (Jimbo *et al.*, 2011b).

However, some studies have shown that the biological outcomes of the same coating do not necessarily show enhanced osseointegration (Svanborg *et al.*, 2011), possibly due to the low sensitivity of the conventional evaluation techniques. Therefore, three-dimensional evaluation by micro-computed tomography has been implemented to obtain further detailed information (Jimbo *et al.*, 2011a). In this study, the effect of nanostructured HA coating

was evaluated histologically. Further, to determine the nanomechanical properties of the bone surrounding the implant, we conducted nanoindentation testing based on the hypothesis that the mechanical aspect of the bone would be improved due to the effect of the nanostructured HA.

MATERIALS & METHODS

Implant Surface Preparation

Twenty threaded implants (Ti6Al4V, $\varnothing 3.3 \times 6$ mm) were used. All implants were sand-blasted and acid-etched (Aadva surface, GC Dental, Tokyo, Japan). Half of the implants (HA) were coated with nano-sized HA according to the Promimic HA$^{nano\text{TM}}$ method (Jimbo *et al.*, 2012). The other half of the implants were subjected to only heat treatment in the same manner as the HA implants (HT).

Morphological Characterization

Surface morphology of the randomly selected implants from each group was examined by scanning electron microscopy (SEM, LEO Ultra 55 FEG, Zeiss, Oberkochen, Germany) at an accelerating voltage of 6 kV (n = 3).

To confirm that the microtopography had not changed due to the nano HA coating, we characterized surface topography by optical interferometry (MicroXam; ADE Phase Shift, Inc., Tucson, AZ, USA). Three implants from each group were randomly selected, and each was measured at 9 regions (3 tops, 3 thread valleys, and 3 flanks).

The parametric calculation was performed after the removal of errors of form and waviness by the use of a Gaussian filter $(50 \times 50$ μm).

Implantation and Sample Preparation

The animal study was approved by the Malmö/Lund (Sweden) regional animal ethics committee (approval number: M282-09). One HA and one HT implant were inserted into the left and right tibias, respectively, of 10 adult Swedish lop-eared rabbits (mean weight, 4.2 kg). The animals were anesthetized with intramuscular injections of a mixture of 0.15 mL/kg medetomidine (1 mg/mL Dormitor; Orion Pharma, Sollentuna, Sweden) and 0.35 mL/kg ketamine hydrochloride (50 mg/mL Ketalar; Pfizer AB, Sollentuna, Sweden). Lidocaine hydrochloride (Xylocaine; AstraZeneca AB, Södertälje, Sweden) was administered as local anesthetic at each insertion site at a dose of 1 mL. After the surgical site exposure, osteotomy was prepared with a series of drills (final diameter, $\varnothing 2.9$), and thereafter, the implants were inserted. Post-operatively, buprenorphine hydrochloride (0.5 mL Temgesic; Reckitt Benckiser, Slough, UK) was administered as an analgesic for 3 days. To observe the early bone formation and to compare the outcomes of the study with those of other studies using the nano HA-coated surface (Svanborg *et al.*, 2011), we chose a time-point of 3 wks.

At 3 wks post-operatively, the rabbits were sacrificed, and the bone samples were retrieved and placed in 4% formaldehyde for 24 hrs; thereafter, they were placed in a series of dehydration and infiltration baths and, finally, were embedded in light-curing resin (Technovit 7200 VLC; Heraeus Kulzer, Wehrheim, Germany).

Ground Sectioning and Histological Analysis

All samples were processed for undecalcified ground sectioning. In brief, the embedded samples were cut in the middle of the implant, and one central undecalcified cut and ground section of approximately 15 μm was prepared and stained with toluidine blue and pyronin G. Histological evaluation was performed by light microscopy (Eclipse ME600; Nikon, Tokyo, Japan), and histomorphometric data were analyzed by Image J (v. 1.43u; National Institutes of Health). The bone-to-implant contact (BIC) along the entire implant was calculated at ×10 to ×40 objective magnification.

Nanoindentation

The remaining resin blocks were processed in the same manner as the histological sections (thickness: approximately 100 μm); for scratch removal, further polishing was performed with diamond suspensions of 9 to 1 μm particle size (Buehler, Lake Bluff, IL, USA). Nanoindentation (n = 28/specimen) was performed with a nanoindenter (Hysitron TI 950, Minneapolis, MN, USA) equipped with a Berkovich diamond three-sided pyramid probe (Baldassarri *et al.*, 2012). A wax chamber was created so that tests were performed in distilled water (Wallace, 2012). A loading profile was developed with a peak load of 300 μN at a rate of 60 μN/sec, followed by a holding time of 10 sec and an unloading time of 2 sec (Fig. 1B). The extended holding period allowed bone to relax to a more linear response, so that no tissue creep effect occurred in the unloading portion of the profile (ISO 14577-4). Therefore, from each indentation, a load-displacement curve was obtained (Fig. 1B; Doerner and Nix, 1986).

For each specimen, mechanical testing was performed in the threaded region (cortical area), in which new bone formation is generally present at early observation time-points. Since interfacial bone modeling and remodeling (and potentially bone kinetics and mechanical properties) have been shown to change as a function of the interplay between surgical instrumentation and implant geometry (Coelho *et al.*, 2010), the region between threads was subdivided into 4 bone quadrants (Fig. 1C). Bone tissue was detected by imaging with light microscopy (Hysitron TI 950, Minneapolis, MN, USA) (Butz *et al.*, 2006), and indentations were performed in the selected areas. From each analyzed load-displacement curve, reduced modulus (GPa) and hardness (GPa) of bone tissue were computed, and elastic modulus Eb (GPa) was calculated as follows:

$$\frac{1}{E_r} = \frac{1-v^2}{E} + \frac{1-v_i^2}{E_i}$$

where Er is the reduced modulus (GPa), ν (0.3) is the Poisson's ratio for cortical bone, and Ei (1140 GPa) and νi (0.07) are the elastic modulus and Poisson's ratio, respectively, for the indenter (Oliver and Pharr, 1992b; Hoffler *et al.*, 2000, 2005).
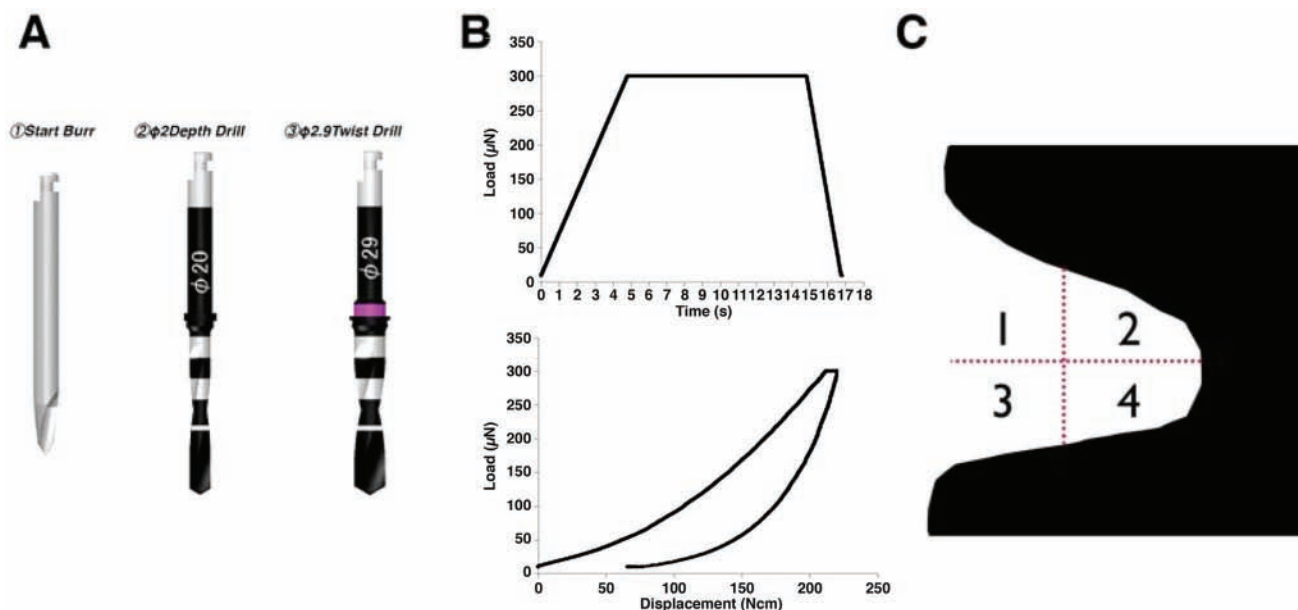
Figure 1. Description of methods used in the study. **(A)** Drill sequence used for implantation. **(B)** Load in *in vivo* time, *quasi*-static testing profile, and a representative load displacement graph of the nanoindentation analysis. **(C)** The region of interest created for the study. The area within the thread was subdivided into 4 quadrants so that we could determine whether area differences exist in the bone nanomechanical properties.

Statistical Analysis

The mean values of surface roughness were compared by one-way ANOVA with the significance level set at 0.05. The non-parametric Wilcoxon signed-rank test was used for bilaterally inserted implants, with the significance level set at 0.05. For nanomechanical testing, we used linear mixed models to determine the influence of different surfaces (HA *vs*. HT) and bone positions within threads (Fig. 1C) on rank elastic modulus and rank hardness values (statistical summaries for the different variables are also presented, but statistical inferences were made based on ranked data).

RESULTS

Morphologic and Topographic Analysis

SEM micrographs of both groups are presented in Figs. 2A-2D. At high magnification, it is evident that the HA-coated surface was fully covered with rod-shaped HA particles approximately 10 to 15 nm wide and 100 to 200 nm long (Fig. 2D).

No significant topographical differences between the 2 groups were seen at the micro-level; thus, it was confirmed that the microtopography was not altered by the nano HA coating (Fig. 2E).

Histomorphometry

The histological sections presented newly formed trabeculae with deeply stained mineralized tissue for both groups after 3 wks of healing, and no visible differences in bone formation could be confirmed (Fig. 3A).

The mean BIC (SD) values for the HT and HA groups are presented in Fig. 3B. In brief, the BICs for the entire threads were 32.1% (9.9) and 35.7% (8.0) for the HT and HA groups, respectively. There were no significant differences between the 2 groups ($p = 0.21$).

Nanoindentation

The mean $\pm$ SE elastic modulus and hardness for the HA group were 6.01 ± 0.40 GPa and 0.29 ± 0.025 GPa, respectively. For the HT group, the mean $\pm$ SE elastic modulus and hardness were 2.69 ± 0.19 GPa and 0.14 ± 0.007 GPa, respectively (Fig. 4A). Significantly higher levels of hardness rank and elastic modulus rank were observed for the HA group relative to the HT group ($H = p < 0.001$; $E = p < 0.001$, Figs. 4B, 4D). No significant differences in the levels of both hardness rank and elastic modulus rank were observed between positions 1 and 4 ($H = p = 0.17$; $E = p = 0.18$, Figs. 4B, 4D). When surface group and position were evaluated altogether, significantly higher values of hardness rank and elastic modulus rank were observed for the HA group relative to the HT group at all positions (Figs. 4C, 4E).

DISCUSSION

The method for determining the degree of osseointegration depends mainly on histology/histomorphometry and biomechanics. However, it has been discussed that these evaluation techniques may not actually capture the entire phenomenon. In particular, when the effects of nanometer structures are evaluated, detailed approaches are essential to clarify their roles during osteogenesis (Jimbo *et al*., 2011a,b). In our previous study, we reported that the presence of HA nanotopography on
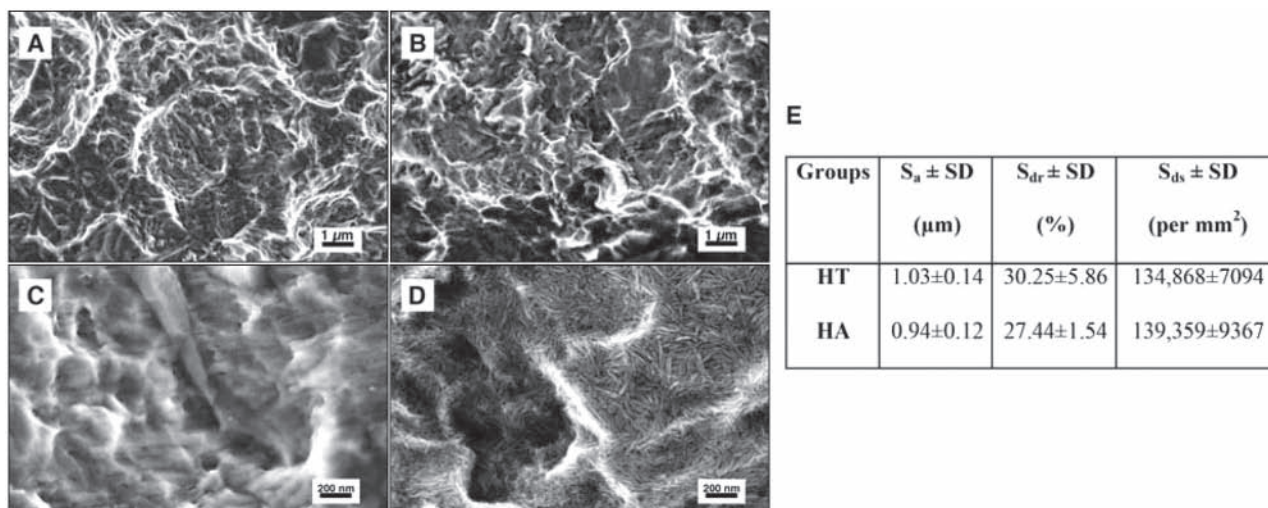
Figure 2. Surface morphologic properties investigated by scanning electron microscopy. Lower magnification images for **(A)** heat-treated (HT) and **(B)** nano hydroxyapatite-coated (HA) implant surfaces. At this magnification (error bars: 1 µm), the rough surface structure of the base substrate can be seen, and it is difficult to see detailed differences between the 2 groups. The higher magnification images (marker bars: 200 nm) clearly indicate differences between the **(C)** HT and the **(D)** HA surfaces. It is evident that the needle-like structure of about 100 nm in length fully covers the HA surface. **(E)** Surface topography measurements conducted by optical interferometry. No statistical differences were detected at the micro-level.

implant surfaces enhanced osteogenic markers, such as alkaline phosphatase and osteocalcin, and, at the same time, suppressed inflammation. It is strongly suggested that chemico-topographical modification at the nano-level enhances bioactivity and osteogenesis, which was difficult to prove with conventional methodologies.

The histomorphometric results of the current study did not show statistical differences between the test and the control surfaces. Both surfaces presented high BIC after 3 wks, which is a time-point commonly selected in a rabbit model to evaluate early bone response (Svanborg *et al.*, 2011). These enhanced histomorphometric outcomes, seen for both surfaces, may be attributed to the base surface topography, which had a moderately rough microtopography (Wennerberg and Albrektsson, 2009). The significant impact of the sand-blasting and acid-etching may have hindered the effects of the nanostructures, at least in the morphometric evaluation. Further, since the coating layer is a monolayer of less than 100 nm, and it is known to metabolize into the living system, remnants of HA particles could not be observed microscopically, and no inflammatory responses were detected, as was the case with thicker HA coatings (Albrektsson, 1998; Reigstad *et al.*, 2011). Thus, qualitatively and quantitatively from a morphologic evaluation, no differences could be detected.
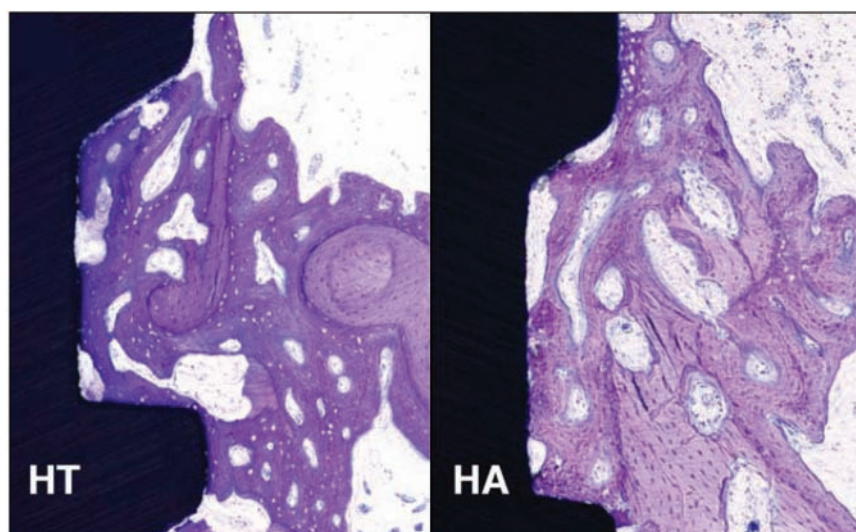
Figure 3. Descriptive histologic images of HT and HA implants placed in the rabbit tibia. For both groups, it was evident that new bone formed from the existing bone and is in contact with the implant surface. No differences between the 2 groups were noted.

Intriguingly, bone nanomechanical testing showed that the tissue properties were uniform throughout the evaluated region (all 4 quadrants) for each group but were significantly enhanced for the HA group relative to the control group. Both the rank elastic modulus and rank hardness presented significantly higher values regardless of different regions, suggesting that the presence of nano HA had an effect at both the immediate interfacial regions and the relatively distant regions. It has been reported that bone nanomechanical properties are strongly correlated to the intrinsic material property of the tissue, *i.e.*, mineralization
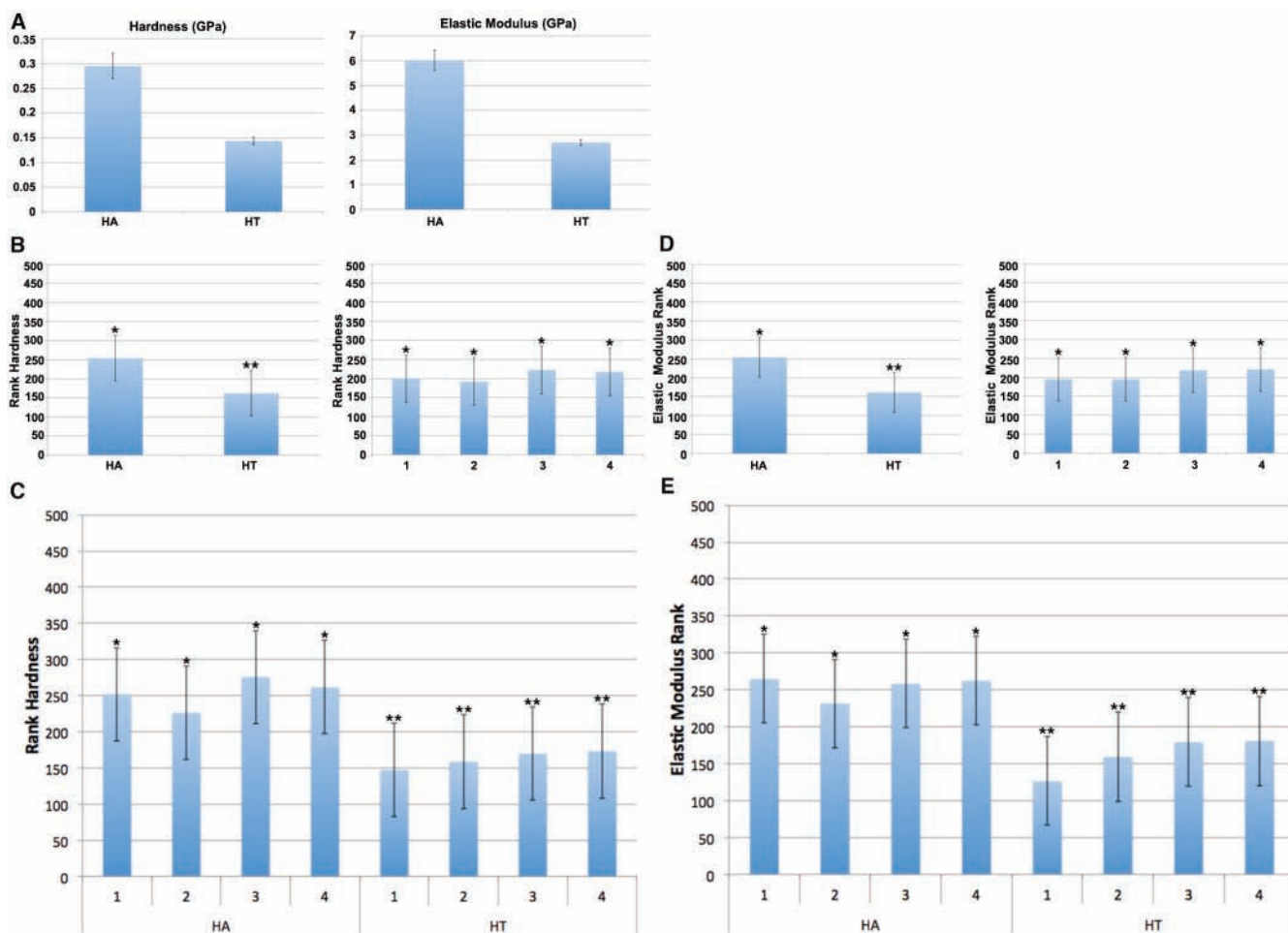
Figure 4. Bar graph representing the results of the nanoindentation. **(A)** Graph representing the mean hardness (GPa) and elastic modulus (GPa) for the HA and HT groups. **(B)** Summary statistics (rank of each property ± 95% confidence interval) for rank hardness as a function of implant surface group and rank hardness as a function of different positions (1-4). **(C)** Rank hardness as a function of implant surface group and different positions (1-4). **(D)** Summary statistics (rank of each property ± 95% confidence interval) for rank modulus as a function of implant surface group and rank modulus as a function of different positions (1-4). **(E)** Rank modulus as a function of implant surface group and different positions (1-4). The number of asterisks depicts statistically homogeneous groups.

of the bone or characteristics of the organic matrix (Currey, 1975; Boivin *et al.*, 2008). More specifically, the calcium content of bone and the Young's modulus have been suggested to have a positive relationship (Currey, 1988). It is a fact that the properties of collagen fibers will be affected by formalin fixation; thus, properties through nanoindentation, while on a larger scale than the collagen fiber level, could be affected. However, since both groups were subjected to the identical fixation process, it is most likely that the 2 groups examined in this study were compared only relatively, and probably not on the basis of absolute bone mechanical properties.

A possible explanation for the higher mineralization could be that the calcium and the phosphate released from the surface had been incorporated into the surrounding new bone, thereby strengthening the mineralization properties. Although, in general, it has been known that hydroxyapatites are the most stable form of the calcium phosphate family, the apatite nanoparticles that were utilized in this study were synthesized according to a

soft-template method (He *et al.*, 2012). According to this method, the apatite formed has a high resemblance to the apatite found in bone, which is a relatively low crystalline, calcium deficient carbonated apatite, with small particle size. Thus, the nano HA used in this study is a soluble form of hydroxyapatite. This phenomenon has been confirmed by Wennerberg *et al.* (2011), who found that radiolabeled [45]Ca coating the implant gradually detached from its surface and was localized in the surrounding new bone, which was eventually metabolized (Wennerberg *et al.*, 2011).

Another possible explanation is the effects of nanostructures enhancing mineralization. As suggested by Tsukimura *et al.*, nanostructured surfaces enhanced the mineralization of rat bone-marrow-derived osteoblasts (Tsukimura *et al.*, 2011). It is suggested that, along with the effect of chemistry, the effect of topography was involved in the enhancement.

Furthermore, the highly active mineralization cascade of the interfacial bone around the nanostructured HA-coated implants

can be explained from a genetic perspective. It has been reported that alkaline phosphatase expression in bone around nanostructured HA-coated implants was significantly higher than that of the bone around non-coated surfaces, and the relative expression differences between the HT and HA surfaces amplified over time (Jimbo *et al*., 2011b). Since high alkaline phosphatase activity enhances osteopontin expression, which is known to be a cohesive factor for mineralization, it is suggested that HA coating was partly responsible for the enhanced bone nanomechanical properties.

Although osseointegration is defined from direct measurement of bone-to-implant contact, the clinical interest today is focusing increasingly on the stability of the implant that will withstand dynamic loading. Clearly, this would require simultaneous new bone formation, and the mineralization level of forming bone may be an essential factor. With the nanoindenter, the capabilities of the nano HA to strengthen bone quality were demonstrated, validating the hypothesis that nanoscale HA-coated implant surfaces will hasten the quality of osseointegration.

While initial bone apposition is an important aspect of osseointegration, longer healing periods, especially when dynamic loading is involved, are of great clinical interest. This study presents purely experimental findings, since only a single 3-week observation was made. Further studies are required to develop conclusions regarding clinical performance.

ACKNOWLEDGMENTS

REFERENCES

Alberts B, Johnson A, Lewis J, Raff M, Roberts K, Walter P (2002). Molecular biology of the cell. New York, NY: Garland Science.

Albrektsson T (1998). Hydroxyapatite-coated implants: a case against their use. *J Oral Maxillofac Surg* 56:1312-1326.

Baldassarri M, Bonfante E, Suzuki M, Marin C, Granato R, Tovar N, *et al*. (2012). Mechanical properties of human bone surrounding plateau root form implants retrieved after 0.3-24 years of function. *J Biomed Mater Res B Appl Biomater* 100B:2015-2021.

Boivin G, Bala Y, Doublier A, Farlay D, Ste-Marie LG, Meunier PJ, *et al*. (2008). The role of mineralization and organic matrix in the microhardness of bone tissue from controls and osteoporotic patients. *Bone* 43:532-538.

Butz F, Aita H, Wang CJ, Ogawa T (2006). Harder and stiffer bone osseointegrated to roughened titanium. *J Dent Res* 85:560-565.

Coelho PG, Suzuki M, Guimaraes MV, Marin C, Granato R, Gil JN, *et al*. (2010). Early bone healing around different implant bulk designs and surgical techniques: a study in dogs. *Clin Implant Dent Relat Res* 12:202-208.

Coelho PG, Freire JN, Granato R, Marin C, Bonfante EA, Gil JN, *et al*. (2011). Bone mineral apposition rates at early implantation times around differently prepared titanium surfaces: a study in beagle dogs. *Int J Oral Maxillofac Implants* 26:63-69.

Currey JD (1975). The effects of strain rate, reconstruction and mineral content on some mechanical properties of bovine bone. *J Biomech* 8:81-86.

Currey JD (1988). The effect of porosity and mineral content on the Young's modulus of elasticity of compact bone. *J Biomech* 21:131-139.

Dalby MJ, Riehle MO, Johnstone HJ, Affrossman S, Curtis AS (2002). Polymer-demixed nanotopography: control of fibroblast spreading and proliferation. *Tissue Eng* 8:1099-1108.

Doerner MF, Nix WD (1986). A method for interpreting the data from depth-sensing indentation instruments. *J Mater Res* 1:601-609.

Ellingsen JE, Johansson CB, Wennerberg A, Holmen A (2004). Improved retention and bone-to-implant contact with fluoride-modified titanium implants. *Int J Oral Maxillofac Implants* 19:659-666.

Goransson A, Arvidsson A, Currie F, Franke-Stenport V, Kjellin P, Mustafa K, *et al*. (2009). An in vitro comparison of possibly bioactive titanium implant surfaces. *J Biomed Mater Res A* 88:1037-1047.

He W, Kjellin P, Currie F, Handa P, Knee CS, Bielecki J, *et al*. (2011). Formation of bone-like nanocrystalline apatite using self-assembled liquid crystals. *Chemistry of Materials* 24:892-902.

Hoffler CE, Moore KE, Kozloff K, Zysset PK, Brown MB, Goldstein SA (2000). Heterogeneity of bone lamellar-level elastic moduli. *Bone* 26:603-609.

Hoffler CE, Guo XE, Zysset PK, Goldstein SA (2005). An application of nanoindentation technique to measure bone tissue lamellae properties. *J Biomech Eng* 127:1046-1053.

Jimbo R, Coelho PG, Vandeweghe S, Schwartz-Filho HO, Hayashi M, Ono D, *et al*. (2011a). Histological and three-dimensional evaluation of osseointegration to nanostructured calcium phosphate-coated implants. *Acta Biomater* 7:4229-4234.

Jimbo R, Xue Y, Hayashi M, Schwartz-Filho HO, Andersson M, Mustafa K, *et al*. (2011b). Genetic responses to nanostructured calcium-phosphate-coated implants. *J Dent Res* 90:1422-1427.

Jimbo R, Sotres J, Johansson C, Breding K, Currie F, Wennerberg A (2012). The biological response to three different nanostructures applied on smooth implant surfaces. *Clin Oral Implants Res* 23:706-712.

Oliver WC, Pharr GM (1992). An improved technique for determining hardness and elastic-modulus using load and displacement sensing indentation experiments. *J Mater Res* 7:1564-1583.

Reigstad O, Johansson C, Stenport V, Wennerberg A, Reigstad A, Rokkum M (2011). Different patterns of bone fixation with hydroxyapatite and resorbable CaP coatings in the rabbit tibia at 6, 12, and 52 weeks. *J Biomed Mater Res B Appl Biomater* 99:14-20.

Svanborg LM, Hoffman M, Andersson M, Currie F, Kjellin P, Wennerberg A (2011). The effect of hydroxyapatite nanocrystals on early bone formation surrounding dental implants. *Int J Oral Maxillofac Surg* 40:308-315.

Tsukimura N, Yamada M, Iwasa F, Minamikawa H, Att W, Ueno T, *et al*. (2011). Synergistic effects of UV photofunctionalization and micro-nano hybrid topography on the biological properties of titanium. *Biomaterials* 32:4358-4368.

Wallace JM (2012). Applications of atomic force microscopy for the assessment of nanoscale morphological and mechanical properties of bone. *Bone* 50:420-427.

Webster TJ, Ahn ES (2007). Nanostructured biomaterials for tissue engineering bone. *Adv Biochem Eng Biotechnol* 103:275-308.

Wennerberg A, Albrektsson T (2009). Effects of titanium surface topography on bone integration: a systematic review. *Clin Oral Implants Res* 20(Suppl 4):172-184.

Wennerberg A, Jimbo R, Allard S, Skarnemark G, Andersson M (2011). In vivo stability of hydroxyapatite nanoparticles coated on titanium implant surfaces. *Int J Oral Maxillofac Implants* 26:1161-1166.